Separation and Purification Technology 278 (2022) 119537

Contents lists available at ScienceDirect

Separation and Purification Technology

journal homepage: www.elsevier.com/locate/seppur

Advanced oxidation processes for removal of organics from cooling tower blowdown: Efficiencies and evaluation of chlorinated species

Pradip Saha [a,b,*], Yicheng Wang [a], Mahsa Moradi [a,c], Robert Brüninghoff [d], Gholamreza Moussavi [c], Bastian Mei [d], Guido Mul [d], Huub H. M. Rijnaarts [a], Harry Bruning [a]

[a] Department of Environmental Technology, Wageningen University and Research, P.O. Box 17, 6700 AA Wageningen, the Netherlands
[b] Department of Chemical Engineering and Polymer Science, Shahjalal University of Science and Technology, Sylhet 3114, Bangladesh
[c] Department of Environmental Health Engineering, Faculty of Medical Sciences, Tarbiat Modares University, Tehran, Iran
[d] Photocatalytic Synthesis Group, MESA+ Institute for Nanotechnology, Faculty of Science and Technology, University of Twente, P.O. Box 217, 7500 AE Enschede, the Netherlands

ARTICLE INFO

Keywords:
Dissolved organic carbon
Humic substances
Saline water
Chlorinated by-products
Advanced oxidation processes

ABSTRACT

One of the major challenges in reusing cooling tower blowdown water (CTBD) utilizing membrane processes is its remaining organic compounds, e.g., humic substances leading to biofouling. Besides, the possible abundance of chloride in CTBD imposes the concern of the formation of chlorinated by-products. To choose a pre-treatment process for the studied CTBD composition, various advanced oxidation processes (AOPs), including electro-oxidation (EO), photocatalytic degradation (PCD), heat-activated persulfate oxidation (PS), UVC/vacuum UV (UVC/VUV), and UVC processes, were evaluated and compared based on two main targets: i) highest removal and mineralization of the organics, especially humic substances; and ii) lowest formation of chlorinated by-products including adsorbable organic halides and oxychlorides. All the processes were conducted in the natural condition of the real CTBD, while solution pH was monitored. Based on results of chemical oxygen demand, total organic carbon, dissolved organic carbon, UV_{254} absorbance, liquid-chromatography–organic carbon detection (LC-OCD), and fluorescence excitation-emission matrices (FEEM), it is concluded that PS leads to complete removal of organic compounds along with the lowest formation of low molecular weight organic acids and organic neutrals. FEEM and LC-OCD data also indicated that EO, PCD, and UVC/VUV processes brought about substantial removal of organic compounds and broke down the humic substances into low molecular weight building blocks and organics. Besides, EO exhibited the highest AOX and oxychlorides formation, while these were limited when using the other AOPs. Summarizing, PS, PCD, and UVC/VUV were efficient processes for the degradation and mineralization of organics without generating significant amounts of chlorinated by-products.

1. Introduction

Water reuse, especially in industrial applications, is highlighted in the sustainable development goals as one of the promising strategies to avoid freshwater scarcity [1]. In many industries, water plays a vital role in energy transportation through a cooling tower [2]. The water is usually supplied from freshwater resources, and several chemicals, e.g., acids, antiscalants and corrosion, and microbial inhibitors, are added as conditioning chemicals. The water becomes concentrated due to evaporation due to the conversion of heat to latent heat. It is discharged as a cooling tower blowdown water (CTBD) to maintain the overall water quality. Thus, the cooling tower blowdown (CTBD) is expected to have high salinity and contains humic substances (HS) and other organic compounds (OCs) in variable concentrations [2]. Löwenberg et al. [3] reported that CTBD from *Dow Benelux B.V.* (the Netherlands) contained 70 to 75% of OCs as HS. There are various treatment approaches for CTBD, and recently, membrane technologies have been studied and applied for the desalination of CTBD streams. However, membrane fouling is still the most concerning and inevitable challenge for reliable membrane performance. Thus, CTBD requires effective pre-treatment before membrane desalination [4]. HS is associated with bio-fouling [5]. G. Amy [5] summarized that different fractions of dissolved

* Corresponding author.
E-mail addresses: pradip.saha@wur.nl, pradip-cep@sust.edu (P. Saha).

https://doi.org/10.1016/j.seppur.2021.119537
Received 30 April 2021; Received in revised form 16 August 2021; Accepted 18 August 2021
Available online 21 August 2021

organic matters (DOM) exhibited organic fouling to both low and high-pressure membranes. Low-pressure processes such as microfiltration or ultrafiltration are commonly used as pre-treatment technologies before application of high-pressure processes, like Nano-filtration or reverse osmosis[6]. However, the microfiltration and ultrafiltration show limited removal efficiency for the dissolved organic fraction, especially the HS, which governs foulant for high-pressure membrane [7]. The application of advanced oxidation processes (AOPs) as a pre-treatment step of membrane processes is a promising approach [8,9]. In AOPs, highly reactive oxidative species (ROS), e.g., hydroxyl radicals ($HO^{\bullet}$) and sulfate radicals ($SO_4^{\bullet-}$), are generated. These ROS attack OCs, including HS from source water, organic additives, microorganisms, etc. [9]. Within the last decade, ozone, H_2O_2, UV, Cl_2, Persulfate, and electrochemical (EO)-based AOPs were studied for mitigating membrane fouling [10]. These studies showed a significant reduction of fouling by HS [8,11–14]. However, the generation of chlorinated organics has been reported as intermediates or by-products of AOPs due to the simultaneous presence of organics, ROS, and reactive chlorine species, e.g., $Cl^{\bullet}$, $Cl_2^{\bullet-}$, Cl_2, or HOCl [15–17]. Furthermore, unfavorable toxic oxychlorides such as ClO^-, ClO_3^- and ClO_4^- have been reported in AOPs due to Cl^- reaction with ROS and reactive chlorine species [18]. In this way, various AOPs exhibit different performances towards producing the above-mentioned chlorinated by-products [19]. For example, photocatalytic degradation (PCD) has been shown to generate significantly fewer chlorinated by-products as compared to electrochemical oxidation (EO) [20]. The ultraviolet light C and vacuum-ultraviolet light (UVC/VUV) study by Moradi et al. [21] for sulfamethoxazole showed that Cl^- reacts with $HO^{\bullet}$ to form $ClOH^{\bullet-}$, which is a transient intermediate and dissociates back to $HO^{\bullet}$. Likewise, oxidation of Cl^- to $ClO_2^{\bullet-}$ by $HO^{\bullet}$ is less probable at pH of 7 while it is viable at acidic conditions. Other studies also showed that UVC/VUV and UVC processes could reduce AOX formation during the oxidation of HS [22]. Hou et al. [18] studied the chlorate formation during the persulfate-based AOPs in the presence of DOC. The study showed that chlorate formation was in forms of $HOCl/OCl^-$ and $SO_4^{\bullet-}$ mediated compounds, which were significantly scavenged by the DOC, eventually inhibiting chlorate formation [18].

Hence, this study focused on OCs removal and chlorinated by-product formation during cooling tower blowdown (CTBD) treatment with different types of AOPs, namely: electrooxidation (EO), photocatalytic degradation (PCD), heat-activated persulfate process (PS), UVC, and UVC/VUV (UVC/VUV) process. Due to the complexity of the water matrix, the performance of the various processes was evaluated by following the chemical oxygen demand (COD), total organic carbon (TOC), dissolved organic carbon (DOC), UV_{254} absorbance, OCs molecular weight distribution by liquid-chromatography–organic carbon detection (LC-OCD) and fluorescence excitation-emission matrices (FEEM) analyses. Organic and inorganic chlorinated by-product formation was monitored by considering adsorbable organic halides and oxychloride species (ClO^-, ClO_3^-, and ClO_4^-). The influence of pH on COD, TOC removal, and by-products formation was also studied.

2. Materials and methods

2.1. Chemicals

Sodium persulfate ($Na_2S_2O_8$, ≥99%), sulfuric acid (H_2SO_4, 95%), sodium hydroxide (NaOH, ≥99%), N,N-diethyl-p-phenylenediamine (DPD, 99%), sodium chloride (NaCl, ≥99%), sodium chlorate ($NaClO_3$, 99%), perchlorate standard for ion chromatography (ClO_4^-, 996 ± 6 mg/L), ethylenediaminetetraacetic acid disodium salt (EDTA, ≥99%), monosodium phosphate (NaH_2PO_4, ≥99%), disodium hydrogen phosphate (Na_2HPO_4, ≥99%), hydrogen peroxide (H_2O_2, 30%), potassium iodide (KI, ≥99%), and uridine ($C_9H_{12}N_2O_6$, ≥99%) were obtained from Merck Chemicals B.V. (the Netherlands).

2.2. Experimental procedure and experimental setup

CTBD used in all the experiments was collected from *Dow* premises in Terneuzen (the Netherlands) and stored at 4 °C to limit microbial growth. The characteristics of the CTBD are given in Table 1 and Table S1. CTBD was filtered through a 110 mm membrane (Whatman, GE Healthcare) before each experiment. pH adjustment was achieved by the addition of concentrated H_2SO_4 (pH 3) or NaOH (pH 10). All experiments were conducted in duplicate, and blank control tests were carried out. All the experiments were conducted for five hours, and the samples were collected at 0 h, 1 h, 2 h, 3.5 h, and 5 h. Free chlorine was measured immediately after the experiment. Samples were kept in a refrigerator at −20 °C for further analysis.

2.2.1. EO experimental setup

The EO experimental setup was described in our previous study [24]. In short, experiments were carried out in an undivided flow cell with a 775 mL/min flow and a reactor volume of 33.6 mL. A boron-doped diamond (BDD) electrode as anode and platinum-coated titanium electrode as a cathode with an effective surface area of 22.4 cm^2 were used (Magneto Special Anodes, the Netherlands). A current density of 8.5 mA/cm^2 was applied for all the EO's experiments using an IviumStat.h potentiostat controlled by Iviumstat software (Ivium Technologies B.V., the Netherlands).

2.2.2. PCD experimental setup

PCD experiments were carried out in a glass beaker. 80 mL CTBD was pre-saturated with air for 20 min before the degradation experiments, and 40 mg (±1) TiO_2 photocatalyst (Hombikat UV100) was added. Pretreatment of TiO_2 photocatalyst, via annealing at 600 °C for 4 h, was performed to achieve an improved photocatalytic performance (optimum between adsorbed surface OH groups and available holes at the surface), as reported in earlier work by our group [20,25]. The catalysts themselves are stable, and additional treatments are generally not required. The beaker was covered with a quartz lid and stirred at 350 rpm in dark conditions for 30 min. UV-irradiation at 375 nm was achieved using a closed box reactor equipped with eight 18 W TL-D UV lamps (Philips). The intensity of the lamp at 375 nm was ≈ 0.32 mW/cm^2 [20]. Samples were centrifuged for 10 min at 8000 rpm to separate the TiO_2 before analysis.

2.2.3. PS experimental setup

The PS experiments were conducted in glass bottles equipped with a pH meter. The temperature was kept at 70 ℃, and the bottles were thoroughly mixed using a shaking water bath (SW23, JULABO GmbH, Germany), oscillating at 150 rpm. CTBD was preheated in the water bath for 30 min and freshly prepared 10 mM PS solution was added into the bottles. During PS activation, H^+ ions are generated, leading to a pH drop [26]. Therefore, a concentrated NaOH solution was added to maintain constant pH during the experiment. Initially, PS was conducted for 5 h. Since the TOC removal changed little after 3 h, all data up to 3 h' reaction was analyzed for PS and compared with other AOPs. Samples were taken and immediately put in an ice bath (<4 ℃) to quench the reaction.

2.2.4. UVC and UVC/VUV experimental setup

The UVC process and UVC/VUV experiments were conducted in

Table 1
Key parameters of cooling tower blowdown (Characteristics are tabulated in detail in Table S1).

Parameter	Unit	Avg. (±SD)
Cl^-	mg/L	467 (3)
TOC	mg/L	47(1)
COD	mg/L	105 (4)

stainless steel 0.3 L annular reactor (400 mm length × 25 inner and 40 mm outer diameters) shown in Fig. S1. A low-pressure mercury UV_{254} lamp for UVC and a $UV_{185/254}$ lamp for UVC/VUV was fixed at the center of the reactor encompassed in a quartz sleeve with 25 mm outer diameter (25 W, Van Remmen UV Technology, the Netherlands). According to H_2O_2 actinometry [27] and uridine actinometry [28], it was estimated that the $UV_{185/254}$ - lamp emitted 8.2 mW/cm^2 intensity at 185 nm and UV_{254} lamp emitted 20.9 mW/cm^2 intensity at 254 nm. Further details of the actinometric methods are given in the supporting information (SI) (text S2, Fig. S2, and Fig. S3). CTBD was recirculated using a peristaltic pump through the reactor at 2 L/min from a circulation bottle. Temperature was kept constant to avoid the influence of elevated temperature on the reaction rate. The CTBD temperature was kept at 25 (±2) °C with cold water recirculation through a cooling coil submersed in the circulation bottle (Fig. S1). Cold water was coming from a water bath (F25-HE, Julabo GmbH, Germany). The lamp and nitrogen stream was turned on 30 min before the experiment to reach the photons' stable output and eliminate the oxygen inside the lamp and quartz sleeve's interspace to prevent ozone formation [29].

2.3. Analytical methods

TOC of the samples was measured by a TOC analyzer (TOC-L CPH/CPN, Shimadzu, Benelux) using the Non-Purgeable Organic Carbon method (text S1.a) [30]. A Hach DR 3900 spectrophotometer (Hach Lange GmbH, Germany) with Hach test kits LCK1414/LCK314 and LCK 390 was used to analyze the COD and AOX, respectively. Dionex ICS-2100 (Thermo, USA) ion chromatography and Perkin Elmer ICP-OES AVIO 500 plasma atomic emission spectroscopy were used for quantification of anions and cations, respectively (text S1.b). PS, H_2O_2, free chlorine, and uridine determination methods are described in the SI (text S1.c) and text S1.d). UV_{254} was measured with an M200 Infinite Pro Microplate Reader (Tecan, Switzerland). The Fluorescence excitation-emission matrix (FEEM) was measured using a Perkin Elmer LS50B fluorimeter (text S1.e). The molecular size distribution of hydrophilic fraction and quantification of hydrophobic fraction of the CTBD's OCs were determined with size-exclusion liquid chromatography (LC-OCD) (Model 8, DOC-Labor, Germany). According to the molecular weight, hydrophilic organics are fractionated into biopolymers (>20000 g/mol), humic substances (~1000 g/mol), low molecular weight (LMW) acid, and LMW neutral (<350 g/mol) (text S2.f) [26].

2.4. Energy consumption calculation

Energy consumption per order can be expressed as $E_{E/O}$ (kWh/m^3), which mean the energy required to remove 90% of the TOC. The following equation can be used to calculate the $E_{E/O}$ [31]:

$$E_{EO} = \frac{P \bullet t}{V \bullet \log\left(\frac{c_i}{c_f}\right)}$$

where P is the energy input in KW, t is the time in h, V is the liquid volume in L, C_i is the initial TOC, and C_f is the final TOC concentration in mg/L. Detailed power consumption calculation is given in SI text S3.

3. Results and discussion

3.1. Evaluation of AOPs for COD and TOC removals

The selected AOPs were applied to remove COD and TOC from the CTBD at pH = 7.4 (±0.3). As shown in Fig. 1, the highest COD removal was obtained by EO, and complete COD removal was observed in 3.5 h. Due to the use of BDD as anode and presence of chloride in the CTBD, both direct/anodic and indirect/mediated electrooxidation have supposedly occurred with synergistic action of ROS and reactive chlorine species for oxidation and mineralization of OCs [20,24,32]. While the highest COD removal was obtained for EO, the EO's efficiency for TOC removal was similar to that of PCD and UVC/VUV processes. Around 50% – 55% TOC removal was obtained. Our previous study on CTBD oxidation with BDD showed that due to partial oxidation and chlorination of the OCs, the oxidation state of the organic carbon was increased and oxygen demand was reduced [24]. A detailed description of this oxidation state phenomenon was reported in [24]. Thus, the TOC removal was lower than COD removal as shown in Fig. 1.

The highest exponential TOC removal (>95%) was obtained using PS. COD removal was not determined for PS due to the interference of PS in COD measurement. In case of PS, O–O bond in PS was homolyzed by heat at 70 °C leading to ROS generation, especially $SO_4^{\bullet-}$ and $HO^{\bullet}$ [33]. Those two radicals have supposedly attacked the OCs of CTBD, leading to a high degree of mineralization. A sufficient amount of persulfate guaranteed abundant formation of ROS to react with organic carbon in the reactor. When lowering the persulfate dose from 10 mM to 5 mM, the TOC removal after 3 h reduced from 83% to 57% (Table S2) in agreement with the results obtained in other similar studies [34,35].

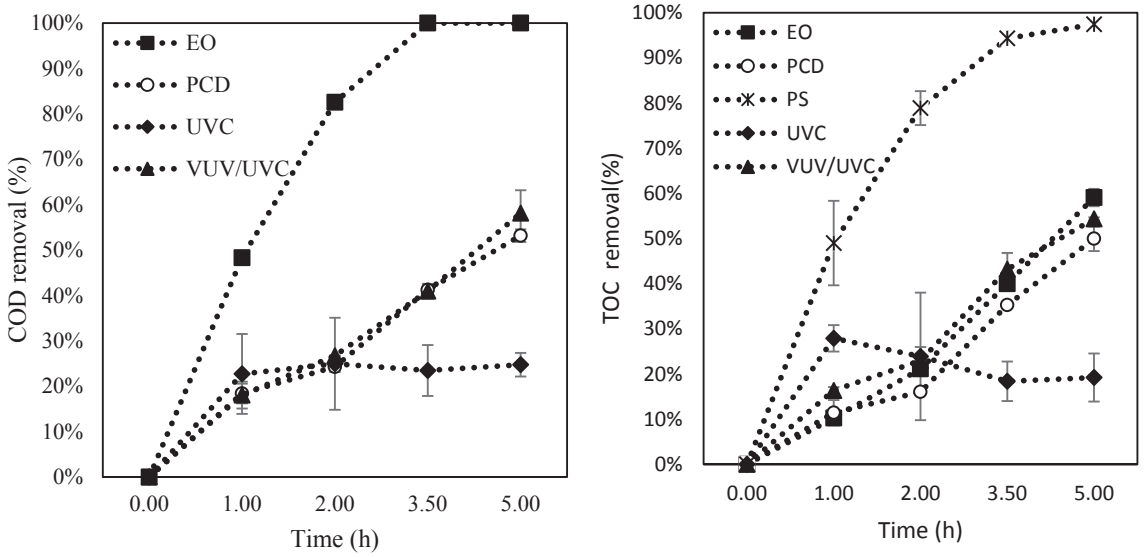

Fig. 1. Removal of: (a) COD and (b) TOC from CTBD during different AOPs:(■) EO with BDD anode at 8.5 mA/cm^2, (◦) PCD with TiO_2 catalyst at 375 nm UV light, (×) PS with 10 mM PS, 70 °C, (◆) UVC/VUV with 185/254 nm UV light, and (▲) UVC with 254 nm UV light, initial pH = 7.4.

During the PCD, COD and TOC removal were up to 55% and 50%, respectively, linearly correlated with time. In PCD, the generation of photo-induced holes (h^+) and electrons (e^-) leads to the occurrence of redox reactions on the heterogeneous solid surface of photocatalyst [36]. Also, various oxidative species, especially the ROS, mainly including $^{\bullet}O_2^-$, H_2O_2, $^1O_2$, and $HO^{\bullet}$ are generated within the solution attacking the OCs ([20,36].

UVC/VUV showed around 58% removal for COD and 53% for TOC, like PCD. In UVC/VUV, organics are attacked/influenced through the following ways [21]: i) homolysis of water molecules when exposed to 185 nm UV and generation of $H^{\bullet}$ and $HO^{\bullet}$; ii) water ionization and generation of free electrons, which are superior for reductive degradation reactions; iii) generation of ozone and H_2O_2; and iv) direct photolysis. As shown in Fig. 1, using the UVC process, merely 25% COD and 19% TOC were removed through direct photolysis after 5 h. An experiment in identical conditions with Milli-Q showed that about 9.0 μM H_2O_2 was accumulated in UVC/VUV, but no H_2O_2 was detected for the UVC process, indicating $HO^{\bullet}$ generation during UVC/VUV (Fig. S2) [37]. With a high oxidation potential of 2.80 V, $HO^{\bullet}$ enhanced the removal efficiency of OCs in UVC/VUV [21]. On the contrary, UV photolysis is efficient only in compounds with a high molar absorption coefficient at the used light source [38]. Compared to the other AOPs, in the UVC process, the OCs removal mainly occurred within the first 1 h, while after that, fluctuations around the average value were observed. A possible explanation could be the limited photolysis ability of UVC light towards the OCs, which reached its maximum value within 1 h. In similar cases of applying UVC, removal capacity has also reached its maximum within one hour [39–42].

3.2. Degradation of the humic substances

3.2.1. Influence of AOPs on UV_{254} removal

UV absorbance at 254 nm (UV_{254}) was determined before and after the treatment, and the results are depicted in Fig. 2. As seen, UVC/VUV brought about the highest UV_{254} removal (85%), although it did not result in the maximum TOC removal. Similarly, the UVC process alone removed 19% of TOC while a 67% UV_{254} reduction was achieved. Unlike TOC, UV_{254} decrease indicates a decline of HS's aromatic and conjugated double bond [43]. These reactions are reported to coincide with a partial breakdown of HS's complex and large molecules to smaller molecules with lower molar absorption coefficients [44]. Research from García et al. [45] also concluded that decreasing specific UV absorption (reduction of aromaticity) was not strictly correlated with HS's complete depletion. In EO, PCD, and PS, the UV_{254} removal efficiencies were ca. 75%. In these processes, the generation of ROS led to the destruction of HS's aromatic content [46].

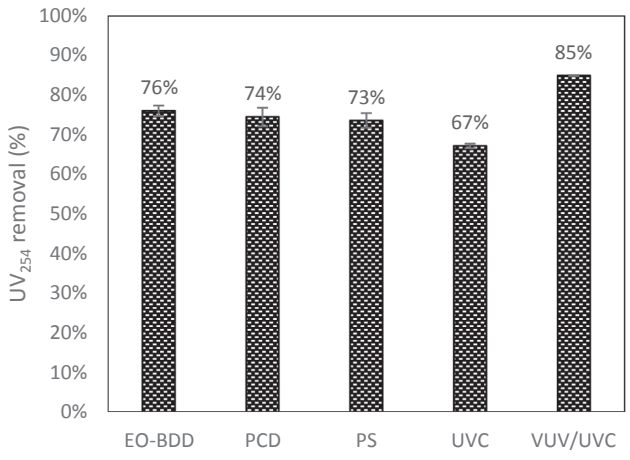

Fig. 2. UV_{254} absorbance removal of the CTBD in various AOPs: (1) EO with BDD anode at 8.5 mA/cm^2 (5 h), (2) PCD with TiO_2 catalyst at 375 nm UV light (5 h), (3) PS with 10 mM PS, 70 °C (3 h), (4) UVC/VUV with 185/254 nm UV light (5 h), and (5) UVC with 254 nm UV light (5 h), initial pH = 7.4.

3.2.2. Change of molecular weight distribution

To follow the DOC molecular weight distribution, LC-OCD analysis was carried out for all AOPs, and corresponding results are shown in Fig. 3 and Fig. S4. The highest DOC removal was observed in PS, by which 35.7 mg/L DOC was removed (80% DOC removal) in 3 h. Indeed, HS was substantially removed, which is desired for the membrane desalination feed water preparation. By EO, a DOC removal of 23.6 mg/L was obtained. Using EO, 19.8 mg/L HS and 1.0 mg/L hydrophobic organic carbon were removed, while 0.5 mg/L LMW acids and 1.4 mg/L LMW organic neutrals were generated as reflected in LC-OCD results. In PCD, 24.0 mg/L DOC involving 25.4 mg/L HS was eliminated, while 3.2 mg/L LMW acids were formed. Applying UVC/VUV, 19.35 mg/L DOC was removed. Although this process exhibited high removal of HS (23.9 mg/L), generations of LMW acids (4.0 mg/L) and organic neutrals (2.6 mg/L) lowered the overall DOC removal. Similarly, in the UVC process, DOC removal was only 10.1 mg/L, whereas HS removal was 13.9 mg/L. Thus, LMW acids and neutrals were formed, lowering the overall DOC removal. Also, LC-OCD chromatogram (Fig. S4) indicated a shoulder peak corresponding to HS's building blocks becoming prominent after the treatment by PCD, EO, UVC/VUC, and UVC process. This building block formation confirms the structural change of the HS and higher UV_{254} removal. Accordingly, LC-OCD analysis showed that even though hydrophobic organic carbon as HS decreased, the concentration of building blocks, LMW acids, and neutrals increased for EO, PCD, UVC/VUV, and UVC process. Such an increase will potentially lead to enhanced biofouling in membrane processes [47]. The PS exhibited efficient DOC removal with no notable formation of LMW acids and neutrals. It is hypothesized that in PS, generation of ROS was sufficient due to the excessive amounts of PS, showing up as the remaining PS after the process (Table S2), resulting in efficient degradation and mineralization of organics.

3.2.3. DOC characterization using FEEM

FEEM, along with LC-OCD and UV_{254}, provides valuable insights into the DOC spectral changes for the studied AOPs. Fluorescence measurements reveal that humic acid (HA)-like, fulvic acid -like, and protein-like HS compounds are present [48,49]. These categories are attributed to DOC's origin, while the variability of these categories represents the degradation status and formation of new fluorophores [50]. The FEEM and fluorescence regional integration (FRI) of FEEM intensity for CTBD before AOPs treatments are presented in Fig. 4a and Fig. 4b. As can be seen, CTBD is mainly comprised of HA and fulvic acid like HS. Thus, the FEEM analysis was consistent with LC-OCD analysis, giving about 33 mg/L HS in initial water samples. The FRI analysis shows that CTBD contains 58% fulvic acid (region III), 27% carboxylic-like HA (region V-i)), and 16% phenolic-like HA (region V-ii). All these HS are capable of causing internal membrane fouling [51]. These HS factions are hardly removed with coagulation/flocculation and powdered activated carbon treatment [3,5].

As shown in Fig. 4b and Table S5, PS exhibited 98% overall FRI intensity removal, which is a valuable output in feed preparation for membrane processes. In the EO, DOC removal was 57%, whereas the overall FRI intensity removal was 97%. This decrease in FRI can be attributed to partial oxidation of the DOC's carbon double bonds and chlorination. Several authors have reported that chlorination of DOC reduces the fluorescence intensity [52,53]. Similarly, PCD, UVC/VUV, and UVC process exhibited 93%, 89%, and 85% overall FRI intensity removal, whereas the DOC removals were 50%, 53%, and 19%, respectively (Table S5).

For all the processes, the overall region's FRI intensity removal was similar to individual region removal for the corresponding AOP (Table S5). Thus, FEEM and UV_{254} results mainly indicate that DOC organic molecular structure changes are reductions in the aromaticity

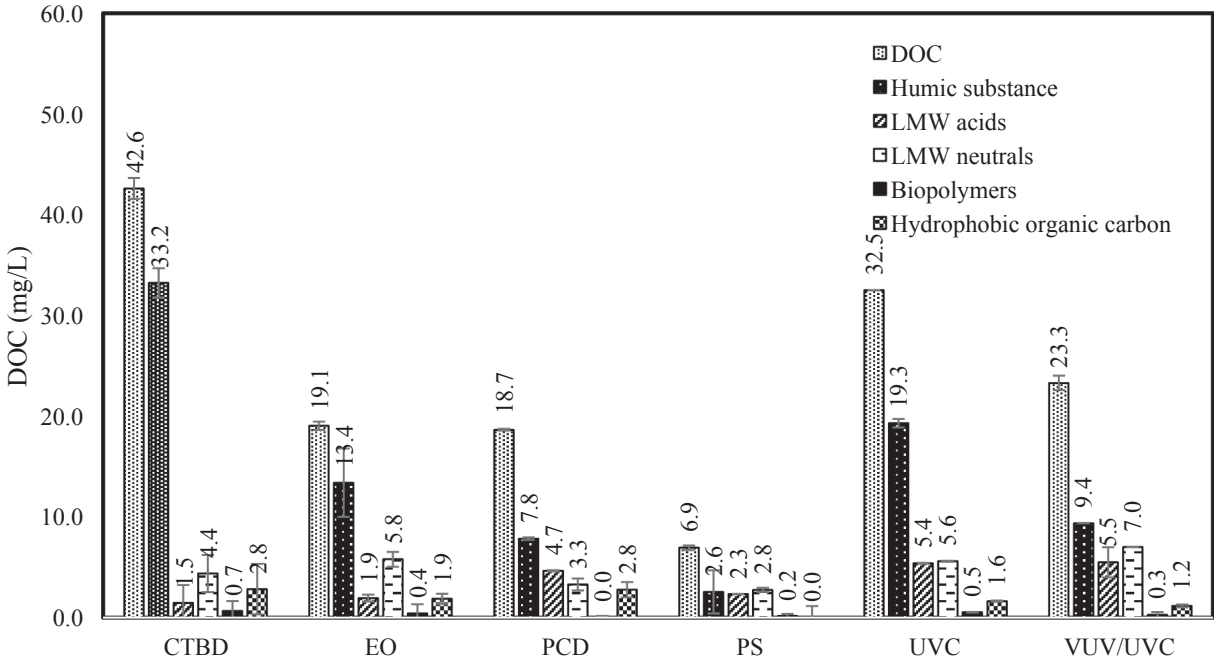

Fig. 3. Speciation of dissolved organic carbon (DOC) of untreated CTBD and after treating CTBD when applying (1) EO with BDD anode at 8.5 mA/cm^2 (5 h), (2) PCD with TiO_2 catalyst at 375 nm UV light (5 h), (3) PS (10 mM), 70 °C (3 h), (4) UVC/VUV with 185/254 nm UV light (5 h), and (5) UVC with 254 nm UV light (5 h), initial pH = 7.4.

and double-bond fractions. So, from the FEEM analyses, it can be concluded that PCD, EO, and UVC/VUV substantially degraded the HS structure to LMW substance, which may cause less internal fouling to the membranes. However, TOC/DOC removal was only around 50 to 55%.

3.3. pH influence on COD and TOC removals in different AOPs

As a parameter that controls oxidation mechanisms, the solution pH effect on the process efficiency was investigated and the results are presented in Fig. 5. The initial and the final pH after treatment are tabulated in Table S3. Variations of the pH may influence the process through: i) chemical speciation of organic and inorganic constituents of the CTBD; ii) speciation of the generated ROS; iii) influencing catalyst's surface reactions in PCD regarding the point of zero charges (pH_{zpc}) and; iv) affecting current efficiency and diffusion rate of substances from the solution to the electrode [54,55]. As can be observed, EO exhibited complete COD removal and around 59% TOC removal independant of the solution pH after 5 h reaction time. The pH influence was limited because the reaction was mass transfer limited [24]. Nevertheless, the other AOPs were dependant on solution pH, especially the UVC/VUV and UVC processes. The UVC/VUV brought about almost complete COD removal and 89% TOC at pH 3, 53, and 45%, respectively, at pH 7 and pH 10 in 5 h. The higher light absorbance of HS caused this high removal efficiency at acidic pH due to the structural change of molecules resulting from protonation [56]. This phenomenon was also confirmed by a 25% increase in COD and TOC removal in the UVC process performed at pH 3 as compared to pH 7. In the UVC process, HS undergoes molecular destruction mainly due to photolysis, while the ROS generation is negligible [57]. The pH value affects HS's speciation and affinity towards photons' absorbance and thereby influences the degradation rate [58]. Using PS, TOC removal efficiencies of ca. 71%, 76%, and 83% were obtained after 3 h, at pH levels of 10, 3, and 7, respectively. pH plays a complex role in heat-activated PS [59,60]. In acidic pH, $SO_4^{\bullet-}$ is the predominant radical, while at pH 9, both $SO_4^{\bullet-}$ and $HO^{\bullet}$ are generated and coexist. When pH exceeds 12, $HO^{\bullet}$ becomes the predominant radical due to the reaction of $SO_4^{\bullet-}$ with hydroxyl ion [59,61,62]. The $SO_4^{\bullet-}$ and $HO^{\bullet}$ reaction mechanisms with OCs are different. For instance, $SO_4^{\bullet-}$ is mainly involved in electron transfer with OCs, while for $HO^{\bullet}$, the reaction mechanism dominantly includes an addition to C = C as well as H abstraction from N-H, C-H, or O-H [59,60]. This difference in the ROS composition and reaction mechanisms is responsible for different TOC removals in the PS at various pH levels. In PCD, TOC removals were increased from 34% to 50% and 55%, respectively; with changing the CTBD pH from acidic to an alkaline condition. The effective degradation in the alkaline environment can be attributed to less inhibition of the TiO_2 catalyst surface due to less effective interaction of the anion species with the negatively charged catalyst surface, and the point of zero charges of TiO_2 is at ~ pH 6 [63–65].

3.4. pH influence on AOX and oxychloride species formation in different AOPs

The influence of initial solution pH on chlorinated organic and inorganic by-products was evaluated. In UVC/VUV, PCD, and UVC process, formation of i) AOX and ii) oxychlorides was negligible (Table 2). Chlorine species (ClO^-/HClO) and chloride radical species are the main precursors of AOX formation [18].

Thus, when the generation of chlorine species is eliminated, the AOX generation is also suppressed [18]. Besides, HS and chloride are both radical sinks, while HS's reaction rate with the radical species is higher than that of the chloride, leading to a lower AOX formation. Also, as indicated in Table 2, zero or negligible amounts of chlorine species were detected after these processes. Thus, AOX formation was suppressed by the absence of one of its major precursors.

However, the EO exhibited significant AOX and chlorine oxyanions formation amongst the studied AOPs independent of pH. AOX formation in EO can be attributed to the simultaneous presence of HS and the high concentration of chlorine species [66,72]. Generally, chlorine evolution is unavoidable at the higher cell potential, leading to reactive chlorine formation. These electro-generated chlorine species react with HS to produce AOX [67,72]. The generated AOX, such as polychlorinated organic compounds, are likely persistent to oxidation; thus, they are not detected by the COD analysis; however, they are measured by TOC/DOC analysis (Fig. 1, Fig. 3 and Fig. 5) [68]. Besides, notable amounts of

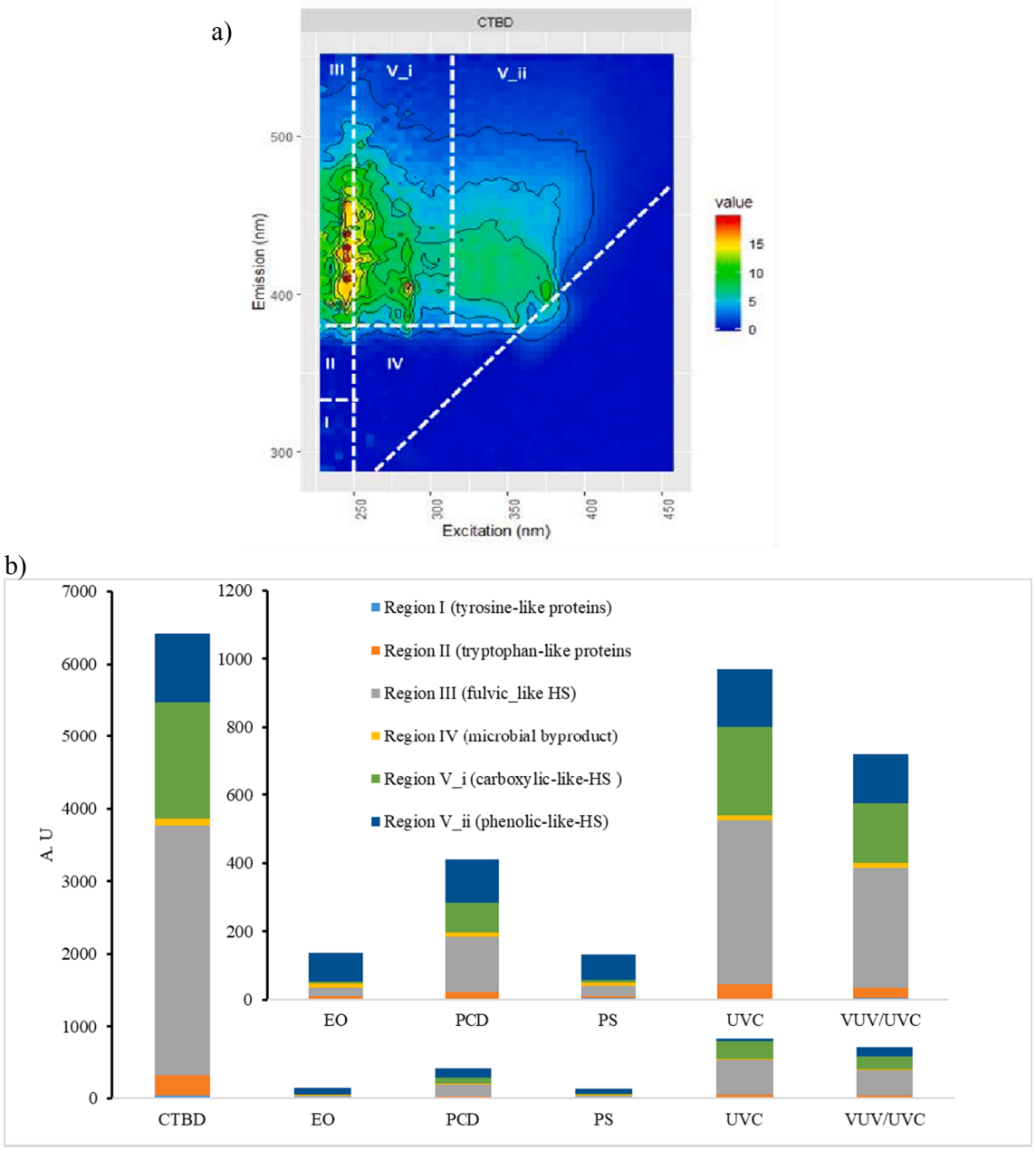

Fig. 4. DOC FEEM profile (a), and (b) FRI intensity of CTBD before and after different AOPs treatments: (1) EO with BDD anode at 8.5 mA/cm^2 (5 h), (2) PCD with TiO_2 catalyst at 375 nm UV light (5 h), (3) PS with 10 mM PS, 70 °C (3 h), (4) UVC/VUV with 185/254 nm UV light (5 h), and (5) UVC with 254 nm UV light (5 h), initial pH = 7.4.

oxychlorides were observed at all pH levels after 5 h EO treatment. The electro-generated chlorine species was accumulated in bulk solution and further oxidized through chain reactions to produce ClO_3^- and ClO_4^-. Using EO, the highest concentrations of AOX were observed at acidic pH of 3, similar to the other studies [68,69]. Another research stated that in alkaline conditions, ClO_3^- concentration increased [69], which was also seen in the study reported here. To sum up, considering complete COD removal at all pH levels but 59% TOC removal along with the high concentration of chlorine oxoanions and AOX in EO; the following subsequent processes mechanism can be assumed to occur in EO: i) direct and ROS mediated oxidation of organics on the high oxygen over-potential BDD anode resulted in degradation of organics; ii) chlorine species accumulated in the system showing up as chlorine oxoanions; iii) formation of persistent AOX as a consequence of chain reactions of OCs and chlorine oxoanions.

As shown in Table 2, in PS, 2.6 mg/L AOX was detected in acidic pH of 3, and a small amount of ClO^- and ClO_3^- were detached at all pH conditions. Yang and co-authors [23] investigated the overestimated adverse effect of halides in the performance of the heat/persulfate process for the degradation of wastewater contaminants. Similarly, they observed few AOX formations and concluded that the heat-activated PS process did not lead to a significant accumulation of AOX in the presence of halides [23]. They stated that in the heat/PS process, $Cl_2^{\bullet-}$ was the primary active chlorinated species when the matrix contained chloride [23].

3.5. Implications for real application

When considering treatment to remove recalcitrant organics from CTBD or similar water, several issues are recommended to be considered

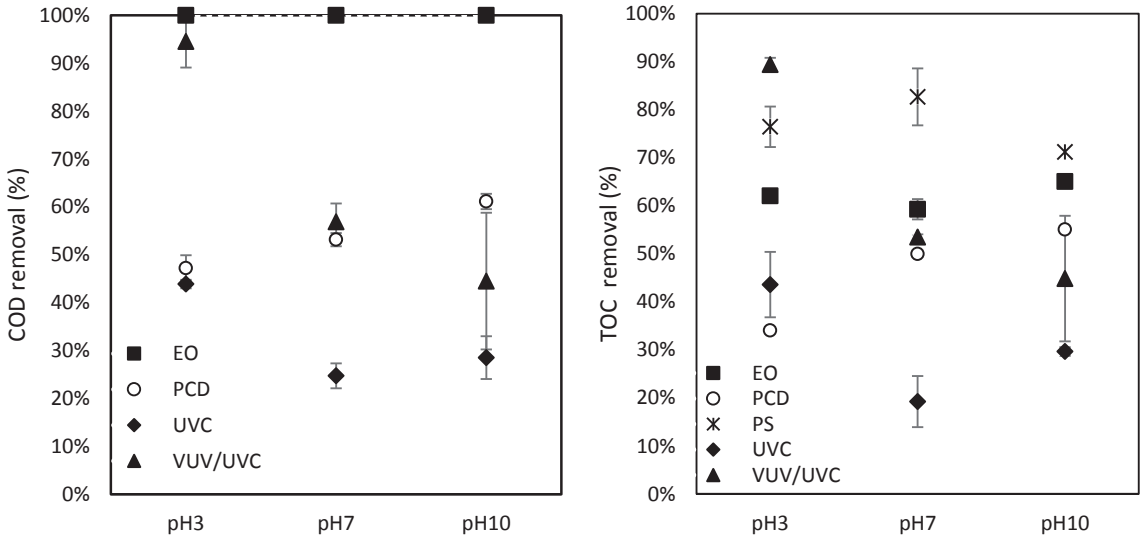

Fig. 5. The influence of pH on (a) COD and (b) TOC removal from CTBD during different AOPs: (■)EO with BDD anode at 8.5 mA/cm^2 (5 h), (○)PCD with TiO_2 catalyst at 375 nm UV light (5 h), (×)PS with 10 mM PS, 70 °C (3 h), (◆)UVC/VUV with 185/254 nm UV light (5 h) (▲)UVC with 254 nm UV light (5 h).

Table 2
Effect of initial solution pH on AOX and inorganic chlorine species during different AOPs of CTBD: (1) EO with BDD anode at 8.5 mA/cm^2 (5 h), (2) PCD with TiO_2 catalyst at 375 nm UV light (5 h), (3) PS with 10 mM PS, 70 °C (3 h), (4) UVC/VUV with 185/254 nm UV light (5 h), and (5) UVC with 254 nm UV light (5 h).

AOPs	pH	ΔCl$^-$ (mg/L)	ΔAOX (mg Cl$^-$/L)	ΔClO$^-$ (mg/L)	ΔClO$_3^-$ (mg/L)	ΔClO$_4^-$ (mg/L)
EO	3	−314 (16)	11.8	160	437(9)	133 (15)
	7	−294 (1)	9.2 (1.0)	210 (10)	459 (2)	149 (2)
	10	−259 (5)	9.5	160	489 (7)	128 (15)
PCD	3	−5 (1)	0.2 (0.1)	ND	ND	ND
	7	−2 (1)	0.2 (0.1)	ND	ND	ND
	10	1 (0.1)	0.1 (0.0)	ND	ND	ND
PS	3	−27 (2)	2.6 (0.1)	0.3 (0.03)	0.7 (0.2)	ND
	7	−16 (0.3)	−0.2 (0.2)	0.2 (0.02)	0.2 (0.2)	ND
	10	−13 (2.5)	−0.1 (0.1)	0.3 (0.05)	0.2 (0.3)	ND
UVC	3	−7	−0.5 (0.1)	ND	ND	ND
	7	−2	−0.2 (0.1)	ND	ND	ND
	10	−9	−0.6 (0.1)	ND	ND	ND
UVC/VUV	3	−2	−0.6 (0.2)	ND	ND	ND
	7	−5	−0.5 (0.1)	ND	ND	ND
	10	−6	−0.7 (0.1)	ND	ND	ND

Notes: ND stands for not detected (below detection limit).

from the application, namely: i) initial characteristics of the matrix and required preparation of the sample (e.g., pH adjustment, OCs removal, etc.); ii) factors associated with the setup and process (reactor design and optimization, ease of operation, etc.); iii) intermediates and by-products; and iv) energy consumption. In Table 3, TOC removal efficiency, energy consumption in terms of $E_{E/0,}$ chlorinated intermediates in terms of AOX and oxychlorides are indicated for each of the studied processes.

As shown in Table 3, in the natural condition of the studied CTBD, the highest TOC removal and the detection of no (insignificant) AOX and oxychlorides were accomplished using PS. To elaborate further, neither

Table 3
Performance of the applied AOPs for the treatment of the studied CTBD. Conditions: (1) EO with BDD anode at 8.5 mA/cm^2 (5 h), (2) PCD with TiO_2 catalyst at 375 nm UV light (5 h), (3) PS with 10 mM PS, 70 °C, (4) UVC/VUV with 185/254 nm UV light (5 h), and (5) UVC with 254 nm UV light (5 h), initial pH = 7.4.

AOPs	TOC removal (%)	oxychlorides	AOX	$E_{E/O}$ (kWh/m^3)
EO	59	High	High	52.6
PCD	50	ND	ND	13.1$^{*/**}$
PS	83 (3 h); > 95 (5 h)	~0	ND	42(5 h) ***
UVC	19	ND	ND	322*
UVC/VUV	53	ND	ND	116*

Notes: ND stands for not detected (below detection limit).
* If the light efficiency is 100% (all the electrical energy converted to corresponding photon energy)
** equivalent energy for TiO_2 production is not included.
*** equivalent energy for PS production is not included.

pH adjustment nor consideration for PS activation was required. PS has an excellent potential to treat CTBD since it can take advantage of the cooling tower's waste heat to activate the persulfate. At the same time, its post-treatment should be carefully designed to remove the extra chemicals added during PS.

UVC/VUV process also fulfilled high TOC removal (89%) merely in acidic pH of 3. This operation at acidic pH necessitates a final polishing step, especially for reuse. Besides, in applying light-induced systems, especially for the treatment of real wastewaters, photon transfer limitations should be overcome [70]. This issue is also controversial for process feasibility in UVC and PCD processes. Using PCD, 50% TOC removal was obtained in the natural pH of the CTBD, although its highest efficiency was marginally higher and was observed at alkaline pH. In this process, AOX and oxychlorides were not detected. However, separation of the catalyst is a notable issue in applying PCD on a full scale, although this can be overcome by developing immobilized heterogeneous catalysts [70,71]. Among the studied processes, EO was the worst in the generation of oxychlorides and AOX, the reasons for which were discussed comprehensively in previous sections. In the presence of chlorine species and HS, EO is not assumed to be a suitable option, leading to the generation of oxoanions of chlorine and AOX in notable concentrations.

For energy consumption, values are calculated for each process as in Table 3. Here, it should be noted that processes were not optimized for

comparison and only considered to evaluate different AOPs for the treatment of a real CTBD under natural conditions concerning OCs removal and the generation of chlorinated intermediates. Overall, amongst the studied AOPs, PS appears to be a promising option for treating matrixes containing OCs and chlorinated species without generating AOX and oxychlorides. It requires 42 kWh/m^3 energy per order of TOC removal. The energy requirement for persulfate activation can be solved using the waste heat from the cooling tower. Obviously, persulfate needs to be supplied continuously, adding cost to the process. EO and PCD also show excellent potential from an energy perspective. They require 52.6 kWh/m^3 and 13.5 kWh/m^3 energy input, respectively. However, BDD anode for EO and TiO_2 catalyst for PCD process would increase the cost.

4. Conclusions

The removal of organic compounds (OCs) from CTBD was carried with electrooxidation (EO), photocatalytic degradation (PCD), heat-activated persulfate oxidation (PS), UVC/vacuum UV (UVC/VUV-AOP), and the UVC process. To assess and compare the treatment efficiency of different AOPs, several parameters were measured: removal of TOC and COD, the concentration of oxoanions of chlorine and AOX, UV_{254}, liquid-chromatography–organic carbon detection (LC-OCD), and fluorescence excitation-emission matrices (FEEM) .

The following conclusions can be drawn based on the experiments:

1. EO, PCD, PS, and UVC/VUV, all removed organic compounds (OCs), while PS provided the highest removal under the experimental conditions chosen.
2. UV_{254} and FEEM results showed that the fraction of humic substance (HS) of the OCs was converted to building blocks and LMW substances, leading to a strongly reduced membrane fouling potential.
3. Acidic conditions strongly favor UVC/VUV treatment performance, explained by an increase of light absorbance, whereas basic conditions favor PCD treatment performance. The pH hardly influences other treatments.
4. AOX and oxychlorides formations were mainly dependent on the formation of reactive chlorine species, which were present, if any, below the detection level of the applied analytical procedure in the UVC, PCD, UVC/VUV, and in insignificant levels in PS.
5. PS could be a suitable method in OCs removal and energy perspective when cooling tower waste heat can be used

Overall, while EO generated chlorinated by-products and chlorinated species-laden solutions, PCD, PS, and UVC/VUVOP demonstrated suitable pre-treatment technologies for the removal of HS/OCs from CTBD and similar waters. Thus PCD, PS, and UVC/VUVOP AOPs before membrane desalination enable reducing membrane fouling effects without significantly forming unwanted chlorinated by-products.

CRediT authorship contribution statement

Pradip Saha: Conceptualization, Methodology, Investigation, Formal analysis, Writing – original draft, Writing – review & editing. **Yicheng Wang:** Investigation, Formal analysis, Writing – original draft. **Mahsa Moradi:** Conceptualization, Writing – original draft, Writing – review & editing. **Robert Brüninghoff:** Conceptualization, Investigation. **Gholamreza Moussavi:** Supervision, Writing – review & editing. **Bastian Mei:** Supervision, Writing – original draft, Writing – review & editing. **Guido Mul:** Supervision, Writing – review & editing. **Huub H. M. Rijnaarts:** Supervision, Writing – review & editing, Funding acquisition. **Harry Bruning:** Conceptualization, Supervision, Writing – original draft, Writing – review & editing.

Declaration of Competing Interest

The authors declare that they have no known competing financial interests or personal relationships that could have appeared to influence the work reported in this paper.

Acknowledgements

This research is financed by the Netherlands Organisation for Scientific Research (NWO), which is partly funded by the Ministry of Economic Affairs and Climate Policy and co-financed by the Netherlands Ministry of Infrastructure and Water Management and partners of the Dutch Water Nexus consortium (project number 14301). Especially, DOW Benelux BV is acknowledged for cooling tower blowdown, MAGNETO special anodes BV is acknowledged for the electrodes, and Van Remmen UV Technology is acknowledged for providing the UV lamps and the quartz sleeves. Tarbiat Modares University and Iran's National Elites Foundation are also acknowledged for the support of Mahsa Moradi during the research stay at Wageningen University and Research.

Appendix A. Supplementary material

Supplementary data to this article can be found online at https://doi.org/10.1016/j.seppur.2021.119537.

References

[1] C. Tortajada, Contributions of recycled wastewater to clean water and sanitation Sustainable Development Goals, npj Clean, Water 3 (1) (2020), https://doi.org/10.1038/s41545-020-0069-3.
[2] X. Yu, H. Yang, H. Lei, A. Shapiro, Experimental evaluation on concentrating cooling tower blowdown water by direct contact membrane distillation, Desalination 323 (2013) 134–141.
[3] J. Löwenberg, J.A. Baum, Y.-S. Zimmermann, C. Groot, W. van den Broek, T. Wintgens, Comparison of pre-treatment technologies towards improving reverse osmosis desalination of cooling tower blow down, Desalination 357 (2015) 140–149.
[4] P.S. Goh, W.J. Lau, M.H.D. Othman, A.F. Ismail, Membrane fouling in desalination and its mitigation strategies, Desalination 425 (2018) 130–155.
[5] G. Amy, Fundamental understanding of organic matter fouling of membranes, Desalination 231 (2008) 44–51.
[6] M.V.N. Mouamfon, W. Li, S.G. Lu, N. Chen, Z.F. Qiu, K.F. Lin, Photodegradation of Sulfamethoxazole Applying UV- and VUV-Based Processes, Water Air Soil Pollut. 218 (2011) 265–274.
[7] W. Zhang, L. Ding, J. Luo, M.Y. Jaffrin, B. Tang, Membrane fouling in photocatalytic membrane reactors (PMRs) for water and wastewater treatment: A critical review, Chem. Eng. J. 302 (2016) 446–458.
[8] S.O. Ganiyu, E.D. van Hullebusch, M. Cretin, G. Esposito, M.A. Oturan, Coupling of membrane filtration and advanced oxidation processes for removal of pharmaceutical residues: A critical review, Sep. Purif. Technol. 156 (2015) 891–914.
[9] J. Zhang, K. Northcott, M. Duke, P. Scales, S.R. Gray, Influence of pre-treatment combinations on RO membrane fouling, Desalination 393 (2016) 120–126.
[10] G.P. Anipsitakis, T.P. Tufano, D.D. Dionysiou, Chemical and microbial decontamination of pool water using activated potassium peroxymonosulfate, Water Res. 42 (2008) 2899–2910.
[11] M. Park, T. Anumol, J. Simon, F. Zraick, S.A. Snyder, Pre-ozonation for high recovery of nanofiltration (NF) membrane system: Membrane fouling reduction and trace organic compound attenuation, J. Membr. Sci. 523 (2017) 255–263.
[12] H.Y. Yen, Fouling Inhibition of Membrane Separation by H2O2/UV Pre-oxidation for Color Filter Effluent Reuse, Ozone Sci. Eng. 38 (2015) 163–171.
[13] R. Gonzalez-Olmos, A. Penadés, G. Garcia, Electro-oxidation as efficient pretreatment to minimize the membrane fouling in water reuse processes, J. Membr. Sci. 552 (2018) 124–131.
[14] B. Liu, F. Qu, H. Yu, J. Tian, W. Chen, H. Liang, G. Li, B. Van der Bruggen, Membrane Fouling and Rejection of Organics during Algae-Laden Water Treatment Using Ultrafiltration: A Comparison between in Situ Pretreatment with Fe(II)/Persulfate and Ozone, Environ. Sci. Technol. 52 (2018) 765–774.
[15] L. Varanasi, E. Coscarelli, M. Khaksari, L.R. Mazzoleni, D. Minakata, Transformations of dissolved organic matter induced by UV photolysis, Hydroxyl radicals, chlorine radicals, and sulfate radicals in aqueous-phase UV-Based advanced oxidation processes, Water Res. 135 (2018) 22–30.
[16] J.D. Garcia-Espinoza, P. Mijaylova-Nacheva, M. Aviles-Flores, Electrochemical carbamazepine degradation: Effect of the generated active chlorine, transformation pathways and toxicity, Chemosphere 192 (2018) 142–151.

[17] A.N. Pisarenko, B.D. Stanford, S.A. Snyder, S.B. Rivera, A.K. Boal, Investigation of the use of Chlorine Based Advanced Oxidation in Surface Water: Oxidation of Natural Organic Matter and Formation of Disinfection Byproducts, J. Adv. Oxid. Technol. 16 (2013) 137–150.
[18] S. Hou, L. Ling, D.D. Dionysiou, Y. Wang, J. Huang, K. Guo, X. Li, J. Fang, Chlorate Formation Mechanism in the Presence of Sulfate Radical, Chloride, Bromide and Natural Organic Matter, Environmental science & technology 52 (2018) 6317–6325.
[19] R. Lamsal, M.E. Walsh, G.A. Gagnon, Comparison of advanced oxidation processes for the removal of natural organic matter, Water Res. 45 (2011) 3263–3269.
[20] R. Bruninghoff, A.K. van Duijne, L. Braakhuis, P. Saha, A.W. Jeremiasse, B. Mei, G. Mul, Comparative Analysis of Photocatalytic and Electrochemical Degradation of 4-Ethylphenol in Saline Conditions, Environ. Sci. Technol. 53 (2019) 8725–8735.
[21] M. Moradi, G. Moussavi, Investigation of chemical-less UVC/VUV process for advanced oxidation of sulfamethoxazole in aqueous solutions: Evaluation of operational variables and degradation mechanism, Sep Purif Technol 190 (2018) 90–99.
[22] C. Hirun-Utok, S. Phattarapattamawong, Degradation and transformation of natural organic matter accountable for disinfection byproduct formations by UV photolysis and UV/chlor(am)ine, Water Sci Technol 79 (2019) 929–937.
[23] F. Yang, B. Sheng, Z. Wang, R. Yuan, Y. Xue, X. Wang, Q. Liu, J. Liu, An often-overestimated adverse effect of halides in heat/persulfate-based degradation of wastewater contaminants, Environ. Int. 130 (2019), 104918.
[24] P. Saha, H. Bruning, T.V. Wagner, H.H.M. Rijnaarts, Removal of organic compounds from cooling tower blowdown by electrochemical oxidation: Role of electrodes and operational parameters, Chemosphere 259 (2020), 127491.
[25] J.T. Carneiro, T.J. Savenije, J.A. Moulijn, G. Mul, Toward a Physically Sound Structure−Activity Relationship of TiO2-Based Photocatalysts, The Journal of Physical Chemistry C 114 (2010) 327–332.
[26] J. Ma, Y.i. Ding, L. Chi, X. Yang, Y. Zhong, Z. Wang, Q. Shi, Degradation of benzotriazole by sulfate radical-based advanced oxidation process, Environ. Technol. 42 (2) (2021) 238–247.
[27] L. Yang, M. Li, W. Li, J.R. Bolton, Z. Qiang, A Green Method to Determine VUV (185 nm) Fluence Rate Based on Hydrogen Peroxide Production in Aqueous Solution, Photochem Photobiol 94 (2018) 821–824.
[28] M.L. Scholes, M.N. Schuchmann, C. von Sonntag, Enhancement of radiation-induced base release from nucleosides in alkaline solution: essential role of the O.- radical, Int J Radiat Biol 61 (4) (1992) 443–449.
[29] K. Zoschke, H. Bornick, E. Worch, Vacuum-UV radiation at 185 nm in water treatment–a review, Water Res. 52 (2014) 131–145.
[30] S.M.T. Raes, L. Jourdin, L. Carlucci, A. vandenBruinhorst, D.P.B.T.B. Strik, C.J. N. Buisman, Water-Based Synthesis of Hydrophobic Ionic Liquids [N8888][oleate] and [P666,14][oleate] and their Bioprocess Compatibility, ChemistryOpen 7 (11) (2018) 878–884.
[31] S. Zhu, B. Dong, Y. Wu, L. Bu, S. Zhou, Degradation of carbamazepine by vacuum-UV oxidation process: Kinetics modeling and energy efficiency, J. Hazard. Mater. 368 (2019) 178–185.
[32] H. Särkkä, A. Bhatnagar, M. Sillanpää, Recent developments of electro-oxidation in water treatment — A review, J. Electroanal. Chem. 754 (2015) 46–56.
[33] S. Wacławek, H.V. Lutze, K. Grübel, V.V.T. Padil, M. Černík, D.D. Dionysiou, Chemistry of persulfates in water and wastewater treatment: A review, Chem. Eng. J. 330 (2017) 44–62.
[34] Y. Ji, C. Dong, D. Kong, J. Lu, Q. Zhou, Heat-activated persulfate oxidation of atrazine: Implications for remediation of groundwater contaminated by herbicides, Chem. Eng. J. 263 (2015) 45–54.
[35] M.-Y. Lee, W.-L. Wang, Y. Du, H.-Y. Hu, N. Huang, Z.-B. Xu, Q.-Y. Wu, B. Ye, Enhancement effect among a UV, persulfate, and copper (UV/PS/Cu2+) system on the degradation of nonoxidizing biocide: The kinetics, radical species, and degradation pathway, Chem. Eng. J. 382 (2020), 122312.
[36] Y. Nosaka, A.Y. Nosaka, Generation and Detection of Reactive Oxygen Species in Photocatalysis, Chem Rev 117 (2017) 11302–11336.
[37] Q. Zhang, L. Wang, B. Chen, Y. Chen, J. Ma, Understanding and modeling the formation and transformation of hydrogen peroxide in water irradiated by 254 nm ultraviolet (UV) and 185 nm vacuum UV (VUV): Effects of pH and oxygen, Chemosphere 244 (2020), 125483.
[38] E. Arany, R.K. Szabo, L. Apati, T. Alapi, I. Ilisz, P. Mazellier, A. Dombi, K. Gajda-Schrantz, Degradation of naproxen by UV, VUV photolysis and their combination, J Hazard Mater 262 (2013) 151–157.
[39] P.B. Moser, B.C. Ricci, C.B. Alvim, A.C.F. Cerqueira, M.C.S. Amaral, Removal of organic matter of electrodialysis reversal brine from a petroleum refinery wastewater reclamation plant by UV and UV/H202 process, J Environ Sci Health A Tox Hazard Subst Environ Eng 53 (2018) 430–435.
[40] T. Wang, Q.-Y. Wu, W.-L. Wang, Z. Chen, B.-T. Li, A. Li, Z.-Y. Liu, H.-Y. Hu, Self-sensitized photodegradation of benzisothiazolinone by low-pressure UV-C irradiation: Kinetics, mechanisms, and the effect of media, Sep Purif Technol 189 (2017) 419–424.
[41] P. Iovino, S. Chianese, S. Canzano, M. Prisciandaro, D. Musmarra, Photodegradation of diclofenac in wastewaters, Desalin. Water Treat 61 (2017) 293–297.
[42] S. Luo, Z. Wei, R. Spinney, Z. Zhang, D.D. Dionysiou, L. Gao, L. Chai, D. Wang, R. Xiao, UV direct photolysis of sulfamethoxazole and ibuprofen: An experimental and modelling study, J Hazard Mater 343 (2018) 132–139.
[43] W. Li, Y. Zhang, P. Zhao, P. Zhou, Y. Liu, X. Cheng, J. Wang, B. Yang, H. Guo, Enhanced kinetic performance of peroxymonosulfate/ZVI system with the addition of copper ions: Reactivity, mechanism, and degradation pathways, J Hazard Mater 393 (2020), 122399.
[44] G. Imoberdorf, M. Mohseni, Degradation of natural organic matter in surface water using vacuum-UV irradiation, J Hazard Mater 186 (2011) 240–246.
[45] A.-M. García, R.A. Torres-Palma, L.A. Galeano, M.Á. Vicente, A. Gil, Separation and Characterization of NOM Intermediates Along AOP Oxidation, in: A. Gil, L. A. Galeano, M.Á. Vicente (Eds.), Applications of Advanced Oxidation Processes (AOPs) in Drinking Water Treatment, Springer International Publishing, Cham, 2017, pp. 99–132.
[46] P. Geng, G. Chen, Antifouling ceramic membrane electrode modified by Magnéli Ti 4 O 7 for electro-microfiltration of humic acid, Sep Purif Technol 185 (2017) 61–71.
[47] L. Chen, P. Cheng, L. Ye, H. Chen, X. Xu, L. Zhu, Biological performance and fouling mitigation in the biochar-amended anaerobic membrane bioreactor (AnMBR) treating pharmaceutical wastewater, Bioresour Technol 302 (2020), 122805.
[48] S. Abdikheibari, L.F. Dumée, V. Jegatheesan, Z. Mustafa, P. Le-Clech, W. Lei, K. Baskaran, Natural organic matter removal and fouling resistance properties of a boron nitride nanosheet-functionalized thin film nanocomposite membrane and its impact on permeate chlorine demand, J. Water. Process. Eng. 34 (2020), 101160.
[49] M. El Kateb, C. Trellu, A. Darwich, M. Rivallin, M. Bechelany, S. Nagarajan, S. Lacour, N. Bellakhal, G. Lesage, M. Heran, M. Cretin, Electrochemical advanced oxidation processes using novel electrode materials for mineralization and biodegradability enhancement of nanofiltration concentrate of landfill leachates, Water Res. 162 (2019) 446–455.
[50] S. Sen Kavurmaci, M. Bekbolet, Tracing TiO2 photocatalytic degradation of humic acid in the presence of clay particles by excitation–emission matrix (EEM) fluorescence spectra, J Photochem. Photobiol. 282 (2014) 53–61.
[51] K. Li, S. Li, C.e. Sun, T. Huang, G. Li, H. Liang, Membrane fouling in an integrated adsorption–UF system: effects of NOM and adsorbent properties, Environ. Sci. Water Res. Technol. 6 (1) (2020) 78–86.
[52] J.R. Lakowicz, Plasmonics in Biology and Plasmon-Controlled Fluorescence, Plasmonics 1 (1) (2006) 5–33.
[53] K.M.H. Beggs, R.S. Summers, D.M. McKnight, Characterizing chlorine oxidation of dissolved organic matter and disinfection by-product formation with fluorescence spectroscopy and parallel factor analysis, J. Geophys. Res. 114 (G4) (2009), https://doi.org/10.1029/2009JG001009.
[54] M. Moradi, G. Moussavi, K. Yaghmaeian, A. Yazdanbakhsh, V. Srivastava, M. Sillanpää, Synthesis of novel Ag-doped S-MgO nanosphere as an efficient UVA/LED-activated photocatalyst for non-radical oxidation of diclofenac: Catalyst preparation and characterization and photocatalytic mechanistic evaluation, Appl. Catal. B 260 (2020) 118128, https://doi.org/10.1016/j.apcatb.2019.118128.
[55] K. Barbari, R. Delimi, Z. Benredjem, S. Saaidia, A. Djemel, T. Chouchane, N. Oturan, M.A. Oturan, Photocatalytically-assisted electrooxidation of herbicide fenuron using a new bifunctional electrode PbO2/SnO2-Sb2O3/Ti//Ti/TiO2, Chemosphere 203 (2018) 1–10.
[56] D.J. Dryer, G.V. Korshin, M. Fabbricino, In situ examination of the protonation behavior of fulvic acids using differential absorbance spectroscopy, Environ Sci Technol 42 (2008) 6644–6649.
[57] G. Moussavi, E. Fathi, M. Moradi, Advanced disinfecting and post-treating the biologically treated hospital wastewater in the UVC/H2O2 and VUV/H2O2 processes: Performance comparison and detoxification efficiency, Process Saf Environ 126 (2019) 259–268.
[58] N. Quici, M.I. Litter, A.M. Braun, E. Oliveros, Vacuum-UV-photolysis of aqueous solutions of citric and gallic acids, J. Photochem. Photobiol. 197 (2008) 306–312.
[59] Y. Fan, Y. Ji, D. Kong, J. Lu, Q. Zhou, Kinetic and mechanistic investigations of the degradation of sulfamethazine in heat-activated persulfate oxidation process, J Hazard Mater 300 (2015) 39–47.
[60] X. Gu, S. Lu, L. Li, Z. Qiu, Q. Sui, K. Lin, Q. Luo, Oxidation of 1,1,1-Trichloroethane Stimulated by Thermally Activated Persulfate, Ind. Eng. Chem. Res. 50 (2011) 11029–11036.
[61] R.H. Waldemer, P.G. Tratnyek, R.L. Johnson, J.T. Nurmi, Oxidation of chlorinated ethenes by heat-activated persulfate: kinetics and products, Environ Sci Technol 41 (2007) 1010–1015.
[62] I.A. Ike, K.G. Linden, J.D. Orbell, M. Duke, Critical review of the science and sustainability of persulphate advanced oxidation processes, Chem. Eng. J. 338 (2018) 651–669.
[63] A.H. Cheshme Khavar, G. Moussavi, A.R. Mahjoub, The preparation of TiO2@rGO nanocomposite efficiently activated with UVA/LED and H2O2 for high rate oxidation of acetaminophen: Catalyst characterization and acetaminophen degradation and mineralization, Appl. Surf. Sci. 440 (2018) 963–973.
[64] K.H. Wang, Y.H. Hsieh, C.H. Wu, C.Y. Chang, The pH and anion effects on the heterogeneous photocatalytic degradation of o-methylbenzoic acid in TiO2 aqueous suspension, Chemosphere 40 (2000) 389–394.
[65] A. Piscopo, D. Robert, J.V. Weber, Comparison between the reactivity of commercial and synthetic TiO2 photocatalysts, J. Photochem. Photobiol. 139 (2001) 253–256.
[66] C. Lutke Eversloh, M. Schulz, M. Wagner, T.A. Ternes, Electrochemical oxidation of tramadol in low-salinity reverse osmosis concentrates using boron-doped diamond anodes, Water Res. 72 (2015) 293–304.
[67] Y. Deng, N. Chen, C. Feng, F. Chen, H. Wang, Z. Feng, Y. Zheng, P. Kuang, W. Hu, Research on complexation ability, aromaticity, mobility and cytotoxicity of humic-like substances during degradation process by electrochemical oxidation, Environ. Pollut. 251 (2019) 811–820.

[68] A.Y. Bagastyo, D.J. Batstone, I. Kristiana, W. Gernjak, C. Joll, J. Radjenovic, Electrochemical oxidation of reverse osmosis concentrate on boron-doped diamond anodes at circumneutral and acidic pH, Water Res 46 (2012) 6104–6112.
[69] C.R. Costa, F. Montilla, E. Morallón, P. Olivi, Electrochemical oxidation of acid black 210 dye on the boron-doped diamond electrode in the presence of phosphate ions: Effect of current density, pH, and chloride ions, Electrochim. Acta 54 (2009) 7048–7055.
[70] F.C. Moreira, R.A.R. Boaventura, E. Brillas, V.J.P. Vilar, Electrochemical advanced oxidation processes: A review on their application to synthetic and real wastewaters, Appl. Catal. B 202 (2017) 217–261.
[71] L. Chen, Y. Jiang, H. Huo, J. Liu, Y. Li, C. Li, N.a. Zhang, J. Wang, Metal-organic framework-based composite Ni@MOF as Heterogenous catalyst for ethylene trimerization, Appl. Catal. A 594 (2020) 117457, https://doi.org/10.1016/j.apcata.2020.117457.
[72] Pradip Saha, Thomas V. Wagner, Jiahao Ni, Alette A.M. Langenhoff, Harry Bruning, Huub H.M. Rijnaarts, Cooling tower water treatment using a combination of electrochemical oxidation and constructed wetlands, Process Saf. Environ. Protect. 144 (2020) 42–51, https://doi.org/10.1016/j.psep.2020.07.019.